

Photogrammetry of a 5m Inflatable Space Antenna With Consumer Digital Cameras

Richard S. Pappa

Senior Research Engineer
Structural Dynamics Branch
NASA Langley Research Center
Hampton, VA 23681

Louis R. Giersch

Graduate Research Assistant
Aerospace & Mechanical Engineering Dept.
George Washington University
Hampton, VA 23681

Jessica M. Quagliaroli

Aerospace Research Summer Scholar
Mechanical Engineering Dept.
University of Connecticut
Storrs, CT 06269

ABSTRACT

This paper discusses photogrammetric measurements of a 5m-diameter inflatable space antenna using four Kodak DC290 (2.1 megapixel) digital cameras. The study had two objectives: 1) Determine the photogrammetric measurement precision obtained using multiple consumer-grade digital cameras and 2) Gain experience with new commercial photogrammetry software packages, specifically PhotoModeler Pro from Eos Systems, Inc. The paper covers the eight steps required using this hardware/software combination. The baseline data set contained four images of the structure taken from various viewing directions. Each image came from a separate camera. This approach simulated the situation of using multiple time-synchronized cameras, which will be required in future tests of vibrating or deploying ultra-lightweight space structures. With four images, the average measurement precision for more than 500 points on the antenna surface was less than 0.020 inches in-plane and approximately 0.050 inches out-of-plane.

INTRODUCTION

NASA is focusing renewed attention on the topic of large, ultra-lightweight space structures. Revolutionary concepts for large antennas and observatories, solar sails, inflatable solar arrays and concentrators, and inflatable habitats, among others, are being studied in NASA's Gossamer Spacecraft Initiative (Refs. 1-3). In the next few years, prototype hardware will be produced and will require structural testing and validation. These systems will use new, ultra-lightweight materials (e.g., carbon nanotubes and membranes with thicknesses less than 5 microns). Their delicate nature requires non-contacting, optical structural measurement techniques. Photogrammetry is a leading candidate technology for this purpose.

Photogrammetry is the science of measuring the dimensions of physical objects using photographs. The classical application of photogrammetry (a.k.a., topographic photogrammetry) is for the making of aerial surveys and maps. More recently, many ground-based applications (a.k.a., non-topographic or close-range photogrammetry) have occurred in such diverse fields as archaeology, architecture, bioengineering, civil engineering, forensic analysis, mechanical inspection, plant engineering, ship construction, and surgery. Close-range photogrammetry is closely affiliated with the technologies of digital image processing and computer vision (Refs. 4-8).

Photogrammetry of ultra-lightweight and inflatable systems will require measurement of structures in one or more of the following three conditions:

- Stationary
- Vibrating
- Deploying

Static shape measurement is the simplest of the three to make, requiring only a few still photographs taken from various directions. Vibration measurements are more difficult since they need time sequences of data and synchronized cameras. With vibrating structures, off-line data analysis is simpler than real-time analysis, which requires special hardware and software and may be limited by computational speed to a few simultaneous measurement points. The most challenging situation of all is the measurement of deploying structures. This case is similar to vibration measurement, but must also handle substantial geometry changes that occur as a function of time.

The research reported in this paper was conducted to begin addressing the technical challenges and requirements of photogrammetry for future, ultra-

lightweight and inflatable space structures. Specific objectives of this work are twofold:

1. Investigate the effectiveness (i.e., accuracy, precision, repeatability, etc.) of photogrammetric measurements of a large, stationary inflatable structure obtained with multiple off-the-shelf consumer digital cameras.
2. Gain experience using various new commercial photogrammetry software packages, specifically PhotoModeler Pro from Eos Systems, Inc. (Ref. 9).[†]

TEST STRUCTURE AND CAMERAS

Figure 1 shows the test article for this project. It is a 5m-diameter inflatable parabolic reflector attached with thin cords at its perimeter to an inflatable Kapton torus with outer diameter of 6.5m and cross-sectional diameter of 0.6m. The total weight of the structure is approximately 4 kg (8.8 lbs). The photograph shows the rear, convex surface of the reflector, which is covered with more than 500 retro-reflective targets for photogrammetry. The other side of the antenna (not visible) has three struts arranged in a tripod configuration for holding the antenna feed.

SRS Technologies of Huntsville, Alabama manufactured this structure for NASA in 1996 under a research and technology development contract. Since then, it has been deflated, folded, moved, and successfully re-inflated many times. This concept can serve in space as either a microwave antenna (radiometer) for earth survey or as a solar concentrator for electrical power generation and/or propulsion (Ref. 10). The shape measurements discussed in the paper were made at room temperature and pressure conditions inside a 16m-diameter vacuum chamber located at the Langley Research Center.

Figure 2 shows one of four Kodak DC290 digital cameras and the specific camera settings used for the photography. This camera creates JPEG or TIFF images with up to 2.1 megapixels of resolution. It was the highest-resolution consumer-grade digital camera available on the market when purchased in late 1999. Features include a built-in flash, 3x zoom lens (focal length of 8 to 24 mm), 2-inch color LCD for image preview, selectable image compression level, and a CompactFlashTM memory card (up to 128 megabytes) for data storage (Ref. 11).

[†]Reference to specific commercial items used in this research is not an official endorsement or promotion of any product by NASA or the United States government.

Four separate DC290 cameras were used to acquire the four photographs in this project. This was done for research purposes. It simulated a future test requirement for photogrammetric measurement of vibrating or deploying structures inside the 16m vacuum chamber using multiple, time-synchronized cameras.

PHOTOGRAMMETRIC ANALYSIS

The basis of photogrammetry is triangulation, whereby the three-dimensional coordinates of objects are calculated knowing the camera locations and the angles between light rays from the objects and the camera image planes (Refs. 4-5). Each point of interest must appear in at least two photographs, although three or more photographs are preferable. Many factors affect photogrammetric accuracy, including: the geometry of objects and camera locations; the number of images and their resolution; exposure and contrast levels of features in the photographs; camera lens characteristics; and the sophistication of the data analysis procedures.

This project used retro-reflective circular targets distributed on the convex side of the antenna. Figure 3 shows a close-up view of a typical target. With the camera flash turned on, each retro-reflective ¼-inch-diameter circle appears in photographs as a bright white ellipse (the elongation of the ellipse depends on viewing angle), which is many times brighter than a diffuse white surface. Surrounded by a black background, this is an ideal photogrammetric target.

The remainder of the paper discusses the eight steps comprising this photogrammetry research project. All camera calibrations and data analyses were performed using the PhotoModeler Pro commercial software package.

Step 1: Calibrate the cameras

Triangulation cannot be done accurately without knowing the internal physical properties of each camera. The process of measuring these properties is called camera calibration. As a minimum, the following data are required for each camera: effective focal length (photogrammetric principal distance), sensor format size, principal point, and lens distortion characteristics. The PhotoModeler software contains a simple procedure for estimating these values by analyzing a grid of targets projected onto a flat wall. These “field” calibration parameters were used in this study. Later, they will be

supplemented with additional calibration information obtained in an instrument research laboratory.

Figure 4 shows a typical set of photos of the camera calibration grid, which is projected onto a flat wall in a darkened room. The grid is a rectangular mosaic of black and white triangles with an overall width/height ratio of 1.5. There are six camera locations and eight photographs. Three locations are on the left side and three on the right side at high, medium, and low elevations. The fourth photograph on each side is taken at medium elevation with the camera rotated by 90 degrees. The user inputs the measured distance from the upper-left to the lower-right corner of the projected image. PhotoModeler then uses a mostly automated procedure to calculate the internal camera parameters from the set of eight photographs.

Tables 1 and 2 show the camera parameters obtained by this approach. To examine the stability of the parameters, each camera was calibrated three times on each of three different days. Table 1 shows the results for Camera 1. Results for the other cameras are similar. It is unknown at this time whether observed fluctuations represent actual physical changes occurring inside the camera(s) or are simply experimental measurement variations. Table 2 shows the average value of each parameter for the nine calibration sessions of each camera. The relative size of the mean values and standard deviations, shown at the bottom of the tables, measures the stability of the parameters. All camera parameters have good repeatability except the P1 and P2 decentering lens distortion values. The large fluctuations of P1 and P2 indicate that they are extremely small quantities (below the measurement capabilities of this calibration technique). When this occurs, Ref. 9 recommends setting them equal to zero in the camera calibration file.

Step 2: Plan the measurements

Planning the measurements primarily involves selecting the number and locations of camera positions for taking the photographs. The inflatable antenna was mounted to a rigid support on the floor near the front wall of the 16m-diameter vacuum chamber. This geometry allowed most camera positions located at least eight meters from the structure to see all of the targets on the convex reflector surface using the full-wide setting of the camera zoom lens.

The baseline data set consisted of four photographs, one from each available camera. Two were taken from a

6m-high scaffold near the back wall of the vacuum chamber on the left and right sides, and two were taken from the floor in approximately the same positions. Ideally, a 90-degree angle between convergent light rays from multiple camera positions is best, but this could not be achieved due to some interference in the chamber. The selected positions provided a vertical camera separation angle of up to 33.6 degrees and a horizontal camera separation angle of up to 58.5 degrees.

Photographic images are inherently non-dimensional (i.e., one cannot tell from photographs of the antenna alone whether it is 10 ft or 100 ft in size). Therefore, two bars of known lengths were included in the scenes for scaling purposes. A 141-3/8-inch horizontal bar was placed in front of the antenna slightly below the reflector surface, and a 104-inch vertical bar was clamped to a stepladder at the left side. Retro-reflective circular targets were placed at the ends of the bars to establish their lengths.

Step 3: Take the photographs

Figure 5 shows the four photographs taken of the 5m inflatable antenna. All photos used a portrait camera orientation to fill the image area as much as possible. The contrast of the retro-reflective targets in the images was maximized by setting the camera flash intensity fully on and turning the vacuum chamber room lights completely off. The resulting photos, used in the data analysis, are underexposed and the structure cannot be clearly seen. (However, the targets appear as bright white ellipses on a predominantly black background, which is ideal.) Figure 5 shows the four images with their brightness and contrast settings artificially increased for improved viewing.

All photography used the camera settings listed in Figure 2. To ensure that the cameras were properly switched to the desired settings (they return to default values when the cameras are turned off), a startup script was written to select these settings automatically. An ASCII script written in the “digita” programming language accomplished this task.

An extremely important feature of close-range photogrammetry is that the user does not need to measure the camera locations or orientations. The software automatically calculates the three spatial coordinates and three orientation angles of each camera if a minimum number of targets (approximately 10 targets or more) appear in overlapping photographs. In PhotoModeler, the

user can display the calculated camera positions and orientations in a graphical 3D viewer for validation of the calculations. A second important feature of close-range photogrammetry, related to the first, is that the cameras do not need to be stationary when the photographs are taken. In particular, the cameras can be vibrating (which includes being handheld). The software accurately calculates the location and orientation of the camera at the instant the photograph is taken, so that camera movement has no effect whatsoever on the photogrammetry results (provided the images are not blurred excessively, which is minimized using a fast shutter speed).

Step 4: Import the photographs into PhotoModeler

The Kodak DC290 camera uses CompactFlash™ memory cards, which are removable solid-state devices about the size of a matchbook. They are available in sizes ranging from 4 to 128 megabytes. Each full-resolution JPEG image requires approximately 400 kilobytes of storage, so that a 96-megabyte memory card, for example, can store over 200 photographs. The images are transferred to a desktop computer for analysis by simply sliding the card out of the camera and inserting it into a peripheral card reader. The images are copied to the computer like floppy disk files are copied. The PhotoModeler software is then started, and the images are imported into the program for analysis.

After opening the images in PhotoModeler, the user associates each image with its specific camera (the cameras can be entirely different types). This association tells the software which internal camera calibration parameters to use when processing the image. Most photogrammetry projects with stationary objects use only one moveable camera, in which case all images are assigned to the same camera. However, in situations where multiple cameras must be used (for example when measuring vibrating or deploying structures) this flexibility in PhotoModeler to associate each photograph with a specific camera description is required.

Step 5: Mark the target locations on each image

The first step of the data analysis is marking the locations of the targets in the images. In other words, the x-y coordinates of the geometric center of every retro-reflective target must be marked as precisely as possible in each image. The circular white targets on the antenna appear in photographs as ellipses of varying size and

aspect ratio depending on the distance and viewing angle of the camera. The x-y target locations are determined in an image-based Cartesian coordinate system.

An important aspect of precision photogrammetry is the availability of sub-pixel interpolation algorithms that can find the center of an ellipse to an accuracy of one-tenth of a pixel or less (Ref. 12). The 3D spatial measurement precision obtained with photogrammetry is directly related to this sub-pixel interpolation factor. For example, the overall three-dimensional measurement precision would improve by approximately a factor of two if the center of each ellipse can be calculated to an accuracy of 1/20 of a pixel rather than to only 1/10 of a pixel. PhotoModeler contains a sub-pixel marking tool for high-contrast circular targets. The targets can be solid light-colored circles on a dark background or vice versa. The software also has the straightforward, non-algorithmic option of marking any distinguishable feature in the images by clicking on it with the mouse, but a human operator is typically only accurate to about one to three pixels.

Figure 6 shows a typical retro-reflective target being marked using the sub-pixel marking tool. The user clicks anywhere near the center of the target and drags the mouse outward until a dashed box encloses the target as shown in Figure 6(a). The software then calculates the boundary of the target and determines its geometric center to sub-pixel resolution using a weighted centroid calculation. The boundary and center are then plotted on the image as shown in Figure 6(b).

In the current release of the PhotoModeler software (Version 3), each target must be marked individually. This was a very time-consuming job in this project with four photographs and over 500 targets. Version 4 of the software will upgrade this tool to perform automatic sub-pixel marking of all targets in a selected region of the image, which will speed up this data analysis step considerably.

Step 6: Identify which points in each image are the same (“Referencing”)

The second step of the data analysis is identifying which marked point in each image is the same physical point on the structure. This process is called “referencing” the points. When a point is initially marked on an image, it is assigned a unique identification number. Then, when a marked point on one image is referenced to

a marked point on another image, the software reassigns the same identification number to both points because they are the same physical location. At the beginning of the data analysis process, the user must perform this referencing operation manually until a certain minimum number of points (approximately 10-15) are referenced on all photos, at which time the user “processes” the data. Processing the data runs a photogrammetric Bundle adjustment algorithm, described in Step 7.

When these calculations finish (typically requires only a few seconds), the user returns to the Referencing operation. Now there is a new, automatic helper tool available to speed up the process. The helper tool is available because processing the data calculated the spatial location and orientation angles of the cameras of the processed images. At this point, the images are said to be “oriented.”

Figure 7 illustrates the use of the referencing helper tool. The user first selects several points in the first image to reference in the other images. These points are the darkened targets in Figure 7(a). The software then automatically moves to each of these points asking the user to reference it in the other photos. For example, in Figure 7 the software is asking the user to reference Point 333. Since the images are oriented, the software can calculate the direction of the light ray from Point 333 to the first camera. It then projects this ray onto the other images. The photogrammetric term for this projected line is an “epipolar line.” PhotoModeler then draws the epipolar line on the second image. This line by itself does not locate the corresponding point in the second photo, but the user knows that the desired point lies somewhere along the line. In most cases this greatly simplifies referencing the point. The long, almost-horizontal line in Figure 7(b) is an example of an epipolar line as it would appear in the second image.

Referencing then becomes much easier once the point is located in the first two photographs. Now, two epipolar lines appear on the third image, corresponding to the projected light rays from the point to each of the first two cameras. Figure 7(b) shows an example of these two intersecting lines appearing on an image. (Note: The second epipolar line appears as a short line segment.) The intersection of the two lines locates the desired point in this image, and the user must simply click the point with the mouse to reference it. In summary, referencing is quite time-consuming on Image 2 because only one epipolar line appears. However, it requires simply clicking on the

points marked by the intersections of two epipolar lines in Images 3 and higher.

In the current release of the PhotoModeler software (Version 3), users must manually click on each point marked by the intersection of two epipolar lines to reference it, which is time-consuming. Version 4 of the software will upgrade this tool to perform fully automatic referencing (once images have been oriented with a minimum number of points), which will speed up this data analysis step considerably.

Step 7: Process the data (Bundle adjustment) and obtain 3D results

The third and final step of the data analysis is to “process” the data using the Bundle adjustment algorithm. In the technical literature, several variations of the Bundle adjustment method appear, with various user options and levels of sophistication (Ref. 13). As discussed in the previous section, the data are processed after approximately 10-15 points have been referenced in all photographs. This orients the images. Then the user returns to referencing additional points. The PhotoModeler user’s guide recommends that the user not reference all of the remaining points at this time, but stop again after adding 20 or so additional points and then re-process the data. Iterating in this way between steps 6 and 7 can avoid wasting a lot of time if for some reason the Bundle adjustment algorithm is unable to successfully handle a large number of additional points (due usually to referencing errors at one or more points). Referencing errors can be located and fixed more easily if only a limited number of new points are re-processed at each step of the procedure.

The Bundle adjustment algorithm does two things simultaneously: 1) Computes the 3D coordinates of all referenced points and estimates their measurement precision and 2) Computes the spatial locations and orientation angles of each camera. The calculations are performed iteratively until a specified number of iterations or consistency is achieved. Iteration is required because the 3D-coordinate calculations use the camera locations and orientations but the camera calculations need the 3D coordinates of the points. In most cases if the set of referenced points is well distributed on the structure, the Bundle adjustment will run successfully.

The data analysis steps described above were followed using the four photographs of the 5m inflatable

antenna. The PhotoModeler software performed exactly as advertised, and the 3D coordinates of all targets were successfully determined using successive Bundle adjustment calculations. A total of 525 points were calculated (521 on the convex surface of the antenna and 4 on the ends of the two scale bars). Following each Bundle adjustment, the camera locations and orientations were plotted using the 3D Viewer available in PhotoModeler. The cameras always appeared in the 3D views to be in the positions that were used to take the photographs, adding assurance that the software was performing properly.

Figure 8 shows the final results of the photogrammetric calculations. This figure is a screen shot of the 3D Viewer with the final set of three-dimensional points and cameras displayed. Unfortunately, it is difficult to see the convex shape of the antenna surface in a two-dimensional plot, but on the computer screen the user can easily rotate, move, or resize this “point cloud,” and it was found to be a well-defined, uniformly curved convex surface as it should be. Using a least-squares analysis, the best parabolic surface representing the complete set of antenna shape measurements was calculated. The focal length of this parabolic surface was 120.09 inches, which compared closely with the design focal length of 120 inches. The root-mean-square (rms) deviation over the entire 5m-diameter reflector surface from an ideal parabolic shape was approximately 1.5 millimeters. Note that Figure 8 shows the four targets located on the ends of the horizontal and vertical scale bars in addition to the 521 targets on the antenna surface.

Table 3 shows the corresponding measurement precisions of the calculated 3D points (at 95% probability). This important information is a by-product of the Bundle adjustment calculations. The overall measurement precision is summarized by the mean values for each of the X, Y, Z directions. (X is horizontal, Y is vertical, and Z is out of the plane of the antenna.) As expected, the X precision is the best because the cameras were more widely separated (closer to 90 degrees) in the horizontal plane than in the vertical plane. The mean value of the Y precision is twice that of the X direction due to this camera geometry. The Z precision is the worst, as expected, because this axis is the most-perpendicular to the image planes of the cameras. The cameras photographed a 6.5m test article; therefore these average precision values correspond to 1:28000 (1 part in 28000)

in the X direction, 1:14000 in the Y direction, and 1:5000 in the Z direction.

The 3D coordinates calculated in this project will be compared soon with additional measurements made during the same testing period (within 15 minutes of each other) using the V-STARS industrial photogrammetry system (Ref. 14). V-STARS uses a professional six-megapixel digital camera and typically achieves a measurement precision of 1:120000, which is several times higher than the values shown in Table 3. For photogrammetry of future vibrating or deploying ultra-lightweight structures in vacuum conditions, which will require multiple synchronized cameras, it may be prohibitively expensive to buy several V-STARS systems because they cost over \$150K each. Also, the outstanding precision of V-STARS may, in fact, be more than what is required for this class of structures. The total cost of the cameras and software used in this study was under \$4K. As consumer digital technology continues to improve, higher-precision cameras than the DC290 should be available soon at a comparable price.

Step 8: Export 3D coordinates to CAD program

Users can export the final three-dimensional target coordinates calculated by PhotoModeler to a CAD program for additional analysis or comparison with design information. Many different file formats are available, including DXF (AutoCAD), 3DS (3D Studio), OBJ (Wavefront), X (Microsoft DirectX), VRML (Virtual Reality Modeling Language), and RAW (raw coordinate data). There are also tools in the software for adding lines, surfaces, and other objects to the three-dimensional model, and these can be exported as well.

One popular use of the data export capability is for creating realistic three-dimensional models of physical objects for posting on the World Wide Web. The VRML file format was specifically designed several years ago for this purpose (Ref. 15). It has both still-life and animation capabilities. Textures extracted from the photographs can be applied to the surfaces of models (a process called “photo-texturing”) to give them a fully realistic visual appearance. Free VRML helper applications are available for most popular web browsers, permitting structural models created with photogrammetry to be quickly and routinely shared with other interested parties anywhere in the world.

CONCLUSIONS

Photogrammetry is a leading candidate technology for measuring the static shape and/or motion of future ultra-lightweight and inflatable space structures. It offers the simplicity of taking photographs coupled with good to excellent measurement precision. This paper discussed recent experiences at NASA using new megapixel consumer digital cameras (Kodak DC290) and commercial photogrammetry software (PhotoModeler Pro) to create a three-dimensional surface model of an inflatable space antenna. PhotoModeler handled this application with ease. This technology can be extended to measure vibrating or deploying structures by analyzing time series of images. Automated, digital photogrammetry is under evaluation as a general shape measurement capability for the 16m-diameter vacuum chamber at the Langley Research Center, where ground tests of additional, ultra-lightweight and inflatable space structures are planned for the months and years ahead.

ACKNOWLEDGEMENTS

The authors extend their thanks to Messrs. Alpheus Burner and Thomas W. Jones of NASA LaRC's Instrumentation Systems Development Branch for photogrammetric technical advice and assistance and to Mr. Tom Burns of NASA LaRC's Quality Applications Technology Branch for making independent measurements of the 5m inflatable antenna with the V-STARS industrial photogrammetry system.

REFERENCES

- [1] "The Gossamer Spacecraft Initiative: Technology to See the Unseen Universe," First Gossamer Workshop, Oxnard, CA, October 1999.
- [2] Chmielewski, A. B., Moore, C., and Howard, R., "The Gossamer Initiative," IEEE paper 0-7803-5846-5/00, January 2000.
- [3] First Gossamer Spacecraft Forum, Held in Conjunction With the AIAA Structures, Structural Dynamics, and Materials Conference, Atlanta, GA, April 2000.
- [4] Church, E. F., *Elements of Photogrammetry*, Syracuse University Press, Syracuse, NY, 1948.

- [5] Karara, H. M., *Handbook of Non-Topographic Photogrammetry*, 2nd edition, American Society of Photogrammetry, Falls Church, VA, 1989.
- [6] Parker, J. R., *Algorithms for Image Processing and Computer Vision*, John Wiley & Sons, New York, NY, 1997.
- [7] Klette, R., Schlüns, K., and Koschan, A., *Computer Vision: Three-Dimensional Data From Images*, Springer-Verlag, Singapore, 1998.
- [8] Russ, J. C., *The Image Processing Handbook*, 3rd Edition, CRC Press, Boca Raton, FL, 1999.
- [9] Eos Systems, Inc., *PhotoModeler Pro User's Manual*, Version 3.1, Vancouver, B.C., Canada, 1999.
- [10] DiChristina, M., "Solar Booster," *Popular Science Magazine*, October 2000, p. 28.
- [11] Kodak Web Site for Digital Cameras & Technology: <http://www.kodak.com/US/en/nav/digital.shtml>.
- [12] West, G. A. W. and Clarke, T. A., "A Survey and Examination of Subpixel Measurement Techniques," in *Close-Range Photogrammetry Meets Machine Vision*, SPIE Proceedings No. 1395, September 1990, pp. 456-463.
- [13] Granshaw, S. I., "Bundle Adjustment Methods in Engineering Photogrammetry," *Photogrammetric Record*, Vol. 10, No. 56, 1980, pp. 181-207.
- [14] Geodetic Services, Inc. Web Site (V-STARS system): <http://www.geodetic.com/>.
- [15] Hartman, J. and Wernecke, J., *The VRML 2.0 Handbook: Building Moving Worlds on the Web*, Addison-Wesley, Reading, MA, 1996.

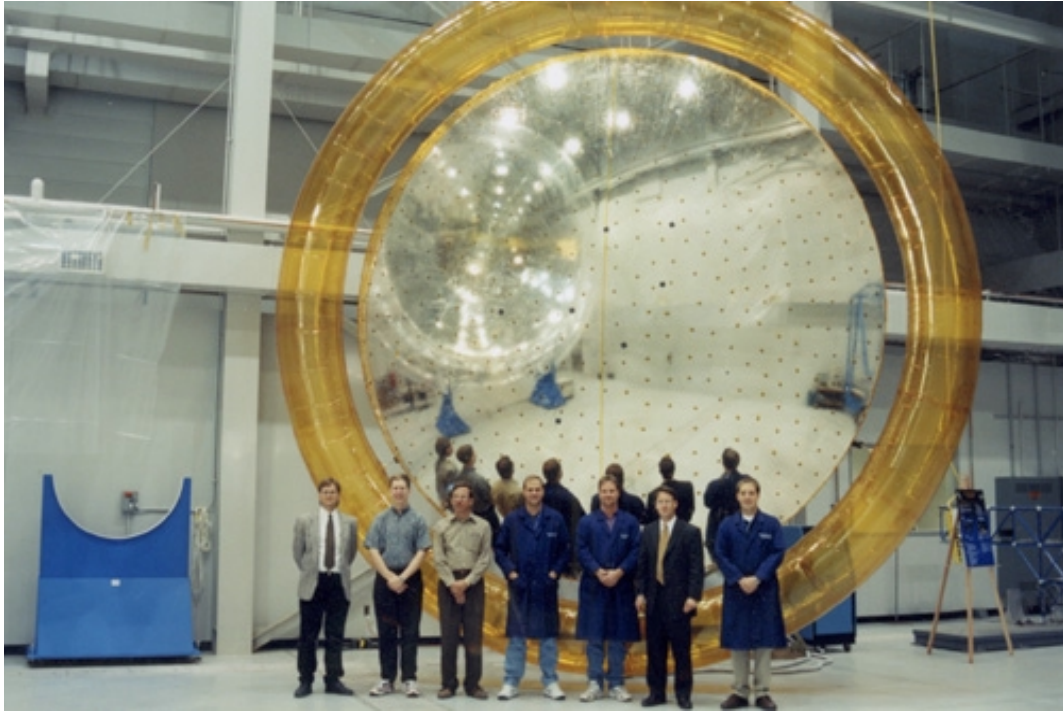
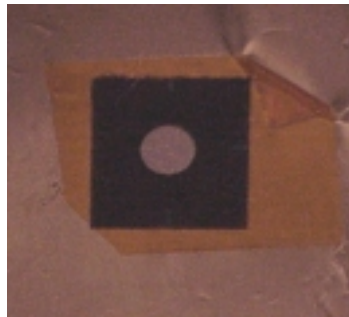


Figure 1 – 5m-Diameter Inflatable Space Antenna

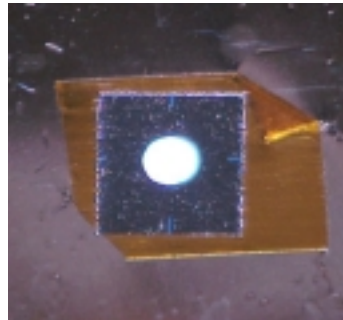


Camera Settings:
 Resolution: 1792 x 1200 pixels
 Quality: Best (least JPEG compression)
 Flash: Fill (always on)
 Zoom: Full wide setting
 White balance: Automatic
 Programmed automatic exposure
 Exposure compensation: 0
 Manual focus distance: 5m

Figure 2 – Kodak DC290 Digital Camera (4 units used in this project)



a) With Camera Flash Turned Off



b) With Camera Flash Turned On

Figure 3 – Close-Up Photographs of Typical Retro-Reflective Target on the Antenna
 (Target Diameter is 0.25 inches)

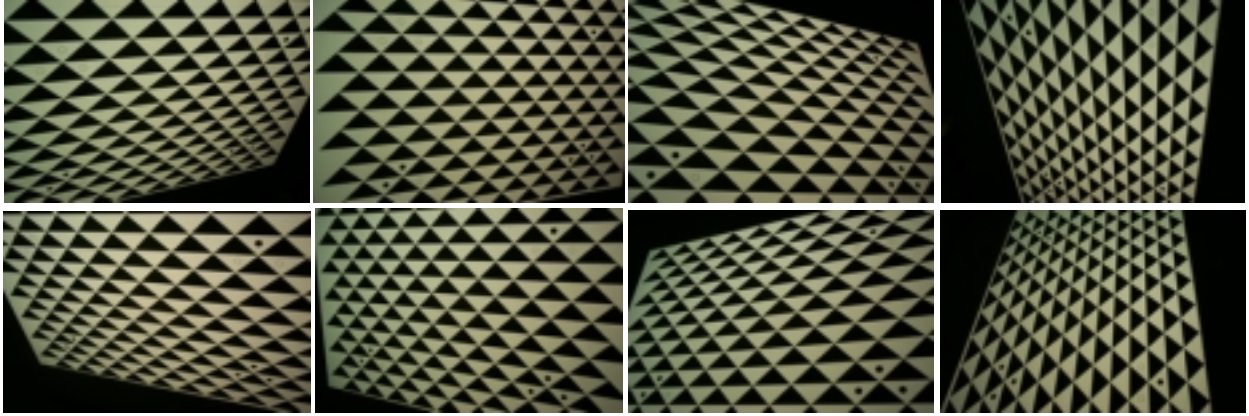


Figure 4 – Camera Calibration Images

Table 1 – Variation of Internal Parameters of Camera 1 for Nine Calibration Sessions

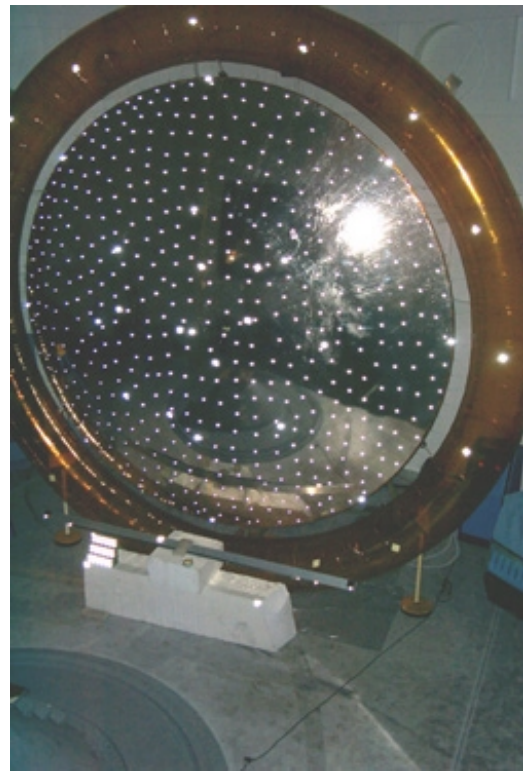
Calibration Session	Focal Length (mm)	Format Size X (mm)	Format Size Y (mm)	Principal Point X (mm)	Principal Point Y (mm)	Radial Lens Distortion		Decentering Lens Distortion	
						K1	K2	P1	P2
Day 1, A	8.228	7.559	5.040	3.813	2.452	1.69E-3	-4.82E-5	-3.90E-5	-31.30E-5
Day 1, B	8.209	7.532	5.040	3.838	2.551	1.82E-3	-4.65E-5	7.05E-5	-7.47E-5
Day 1, C	8.199	7.533	5.040	3.855	2.544	1.73E-3	-3.98E-5	-2.06E-5	-5.87E-5
Day 2, A	8.187	7.532	5.040	3.823	2.565	1.70E-3	-4.00E-5	2.97E-5	0.16E-5
Day 2, B	8.202	7.533	5.040	3.851	2.546	1.79E-3	-4.73E-5	-4.74E-5	-7.82E-5
Day 2, C	8.201	7.533	5.040	3.847	2.544	1.72E-3	-3.89E-5	-1.29E-5	-10.59E-5
Day 3, A	8.198	7.536	5.040	3.849	2.535	1.75E-3	-4.25E-5	2.94E-5	-6.11E-5
Day 3, B	8.202	7.534	5.040	3.852	2.543	1.74E-3	-4.10E-5	0.02E-5	-9.69E-5
Day 3, C	8.203	7.537	5.040	3.848	2.549	1.72E-3	-4.02E-5	2.68E-5	-5.71E-5
Mean:	8.203	7.537	5.040	3.842	2.537	1.74E-3	-4.27E-5	0.41E-5	-9.38E-5
Std. Deviation:	0.011	0.009	0.000	0.014	0.033	0.04E-3	0.36E-5	3.82E-5	8.77E-5

Table 2 – Average Calibration Parameters of Cameras
(Mean Values of Nine Calibration Sessions for Each Camera)

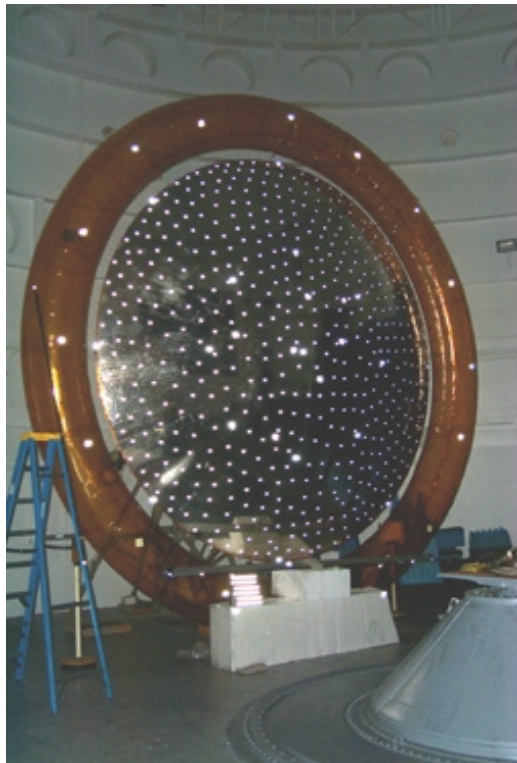
Camera Number	Focal Length (mm)	Format Size X (mm)	Format Size Y (mm)	Principal Point X (mm)	Principal Point Y (mm)	Radial Lens Distortion		Decentering Lens Distortion	
						K1	K2	P1	P2
Camera 1	8.203	7.537	5.040	3.842	2.537	1.74E-3	-4.27E-5	0.41E-5	-9.38E-5
Camera 2	8.206	7.532	5.040	3.888	2.349	1.55E-3	-4.10E-5	-13.70E-5	-4.19E-5
Camera 3	8.181	7.531	5.040	3.822	2.420	1.63E-3	-4.47E-5	-0.97E-5	0.03E-5
Camera 4	8.232	7.533	5.040	3.843	2.504	1.62E-3	-4.18E-5	-2.46E-5	-9.18E-5
Mean:	8.206	7.533	5.040	3.849	2.453	1.64E-3	-4.26E-5	-4.18E-5	-0.71E-5
Std. Deviation:	0.021	0.003	0.000	0.028	0.085	0.08E-3	0.16E-5	6.45E-5	6.07E-5



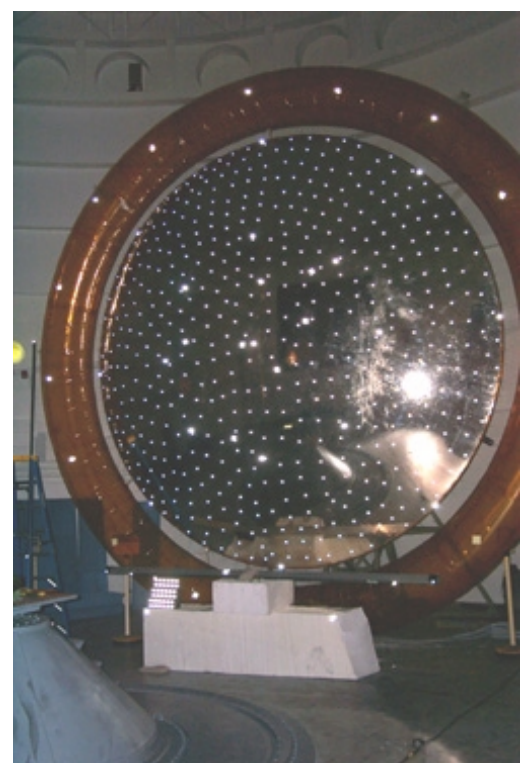
a) Upper-Left Camera Position (Camera 1)



b) Upper-Right Camera Position (Camera 2)

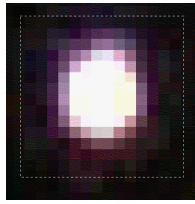


c) Lower-Left Camera Position (Camera 3)

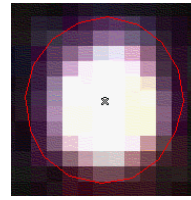


d) Lower-Right Camera Position (Camera 4)

Figure 5 – Images Used in the Photogrammetric Analysis

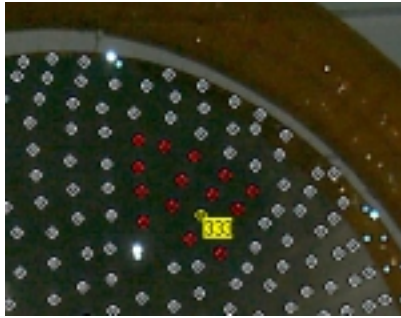


a) Marking the Approximate Boundary of a Target

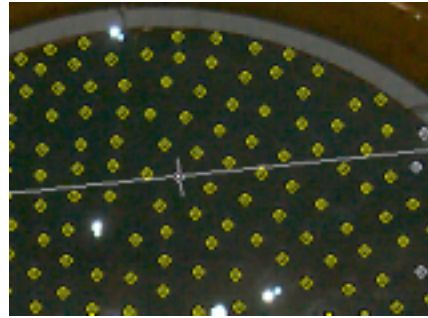


b) Centroid Calculated by Software

Figure 6 – Typical Sub-Pixel Centroid Calculation



a) Select a New Point in Image 1



b) Software Draws Epipolar Line(s) in the Other Images

Figure 7 – Automatic Referencing Using Viewing Rays from Other Cameras

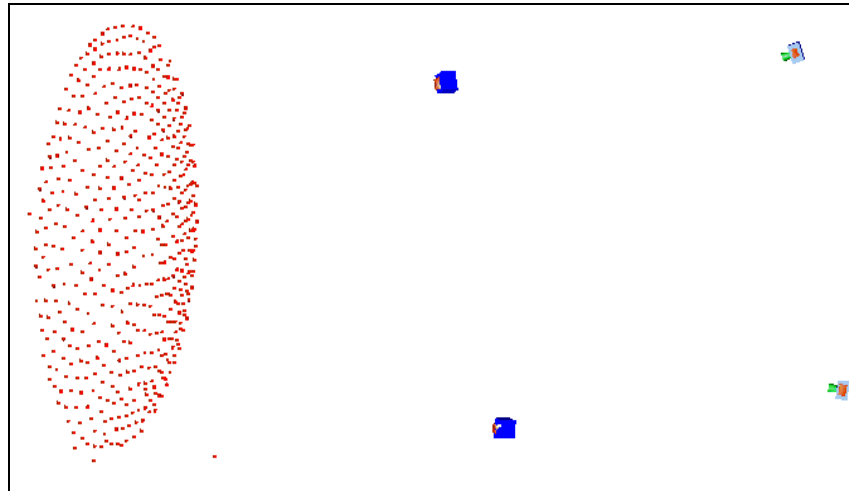


Figure 8 – Final Three-Dimensional Target Locations and Camera Positions Displayed in the 3D Viewer

Table 3 – Measurement Precision in Inches for the 521 Targets on the Antenna

Direction	Minimum	Maximum	Mean	Std. Dev.
X (horizontal)	0.003	0.023	0.009	0.004
Y (vertical)	0.015	0.041	0.018	0.004
Z (out of plane)	0.037	0.112	0.052	0.024
Root-sum-square:	0.040	0.121	0.056	0.025